Stem Cell Reports
Report
ISSCR
OPEN ACCESS

Generating functional cells through enhanced interspecies chimerism with human pluripotent stem cells

Yanling Zhu,[1,2,4,6] Zhishuai Zhang,[1,3,4,6] Nana Fan,[1,4,6] Ke Huang,[1,4] Hao Li,[1,4] Jiaming Gu,[1,3,4] Quanjun Zhang,[1,4] Zhen Ouyang,[1,4] Tian Zhang,[1,4] Jun Tang,[1,4,5] Yanqi Zhang,[1,3,4] Yangyang Suo,[1,4] Chengdan Lai,[1,4] Jiaowei Wang,[1,4] Junwei Wang,[1,4] Yongli Shan,[1,4] Mingquan Wang,[1,4,5] Qianyu Chen,[1,4] Tiancheng Zhou,[1,4] Liangxue Lai,[1,3,4,*] and Guangjin Pan[1,2,3,4,*]

[1]CAS Key Laboratory of Regenerative Biology, Centre for Regenerative Medicine and Health, Hong Kong Institute of Science and Innovation, Guangzhou Institutes of Biomedicine and Health, Chinese Academy of Sciences, Guangzhou 510530, China
[2]Institute for Stem Cell and Regeneration, Chinese Academy of Sciences, Beijing 100101, China
[3]University of Chinese Academy of Sciences, Beijing 100049, China
[4]Guangdong Provincial Key Laboratory of Stem Cell and Regenerative Medicine, South China Institute for Stem Cell Biology and Regenerative Medicine, Guangzhou Institutes of Biomedicine and Health, Chinese Academy of Sciences, Guangzhou 510530, China
[5]Joint School of Life Sciences, Guangzhou Institutes of Biomedicine and Health, Chinese Academy of Sciences, Guangzhou Medical University, Guangzhou 510530, China
[6]These authors contributed equally
*Correspondence: pan_guangjin@gibh.ac.cn (G.P.), lai_liangxue@gibh.ac.cn (L.L.)
https://doi.org/10.1016/j.stemcr.2022.03.009

SUMMARY

Obtaining functional human cells through interspecies chimerism with human pluripotent stem cells (hPSCs) remains unsuccessful due to its extremely low efficiency. Here, we show that hPSCs failed to differentiate and contribute teratoma in the presence of mouse PSCs (mPSCs), while MYCN, a pro-growth factor, dramatically promotes hPSC contributions in teratoma co-formation by hPSCs/mPSCs. MYCN combined with BCL2 (M/B) greatly enhanced conventional hPSCs to integrate into pre-implantation embryos of different species, such as mice, rabbits, and pigs, and substantially contributed to mouse post-implantation chimera in embryonic and extra-embryonic tissues. Strikingly, M/B-hPSCs injected into pre-implantation *Flk-1*$^{+/-}$ mouse embryos show further enhanced chimerism that allows for obtaining live human CD34^{+} blood progenitor cells from chimeras through cell sorting. The chimera-derived human CD34^{+} cells further gave rise to various subtype blood cells in a typical colony-forming unit (CFU) assay. Thus, we provide proof of concept to obtain functional human cells through enhanced interspecies chimerism with hPSCs.

INTRODUCTION

Interspecies chimerism using human pluripotent stem cells (hPSCs) is a promising approach for the generation of xenogenic organs through animal blastocyst complementation (Kobayashi et al., 2010; Isotani et al., 2011; Mascetti and Pedersen 2016, Wu et al., 2017; Das et al., 2020). The strategy that *Pdx1*-deficient murine blastocysts are injected with wild-type rat PSCs has been shown to generate fully functional pancreas tissue of rat origin (Kobayashi et al., 2010). However, hPSCs exhibit very limited efficiency in interspecies chimerism even though they can self-renew and are pluripotent, generating a large variety of cell types upon differentiation *in vitro* and teratoma formation *in vivo* (Thomson et al., 1998; James et al., 2006; Masaki et al., 2015; Wu et al., 2017). One explanation for this limited efficiency is that conventional hPSCs are in a primed state and thus do not match the developmental stage of the pre-implantation blastocyst (Brons et al., 2007; Tesar et al., 2007; Huang et al., 2012; Kojima et al., 2014; Mascetti and Pedersen 2016). To overcome this barrier, intensive efforts have been made to generate naive hPSCs with cellular and transcriptional properties similar to those of naive pluripotent cells (Buecker et al., 2010; Hanna et al., 2010; Chan et al., 2013; Gafni et al., 2013; Takashima et al., 2014; Theunissen et al., 2014; Ware et al., 2014; Guo et al., 2016). However, these naive hPSCs generated by different protocols are highly variable in terms of the efficiency in interspecies chimerism (Gafni et al., 2013; Masaki et al., 2015; Theunissen et al., 2016; Hu et al., 2020), indicating that additional barriers remain to be illuminated. Indeed, we have shown that the conventional hPSCs undergo rapid apoptosis when injected into pre-implantation blastocysts, in part due to activation of the *Ink4a* pathway (Wang et al., 2017a; Huang et al., 2018). Consistently, overexpression of BMI1, which suppresses *Ink4a* or BCL2 to directly inhibit apoptosis, enables primed hPSCs to integrate into the early embryos of mice, rabbits, and pigs and to differentiate into both embryonic and extra-embryonic cell types in mouse chimeras (Wang et al., 2017b; Huang et al., 2018). Recently, Wu et al. reported a cell competition between hPSCs and host cells in interspecies chimerism, which leads to hPSC apopotosis during chimera (Zheng et al., 2021). However, even though apoptosis is blocked in hPSCs by an anti-apoptotic factor such as BCL2 or BMI1, the chimera efficiency is still extremely low, and obtaining live and functional hPSC-derived cells in chimera remains unsuccessful.

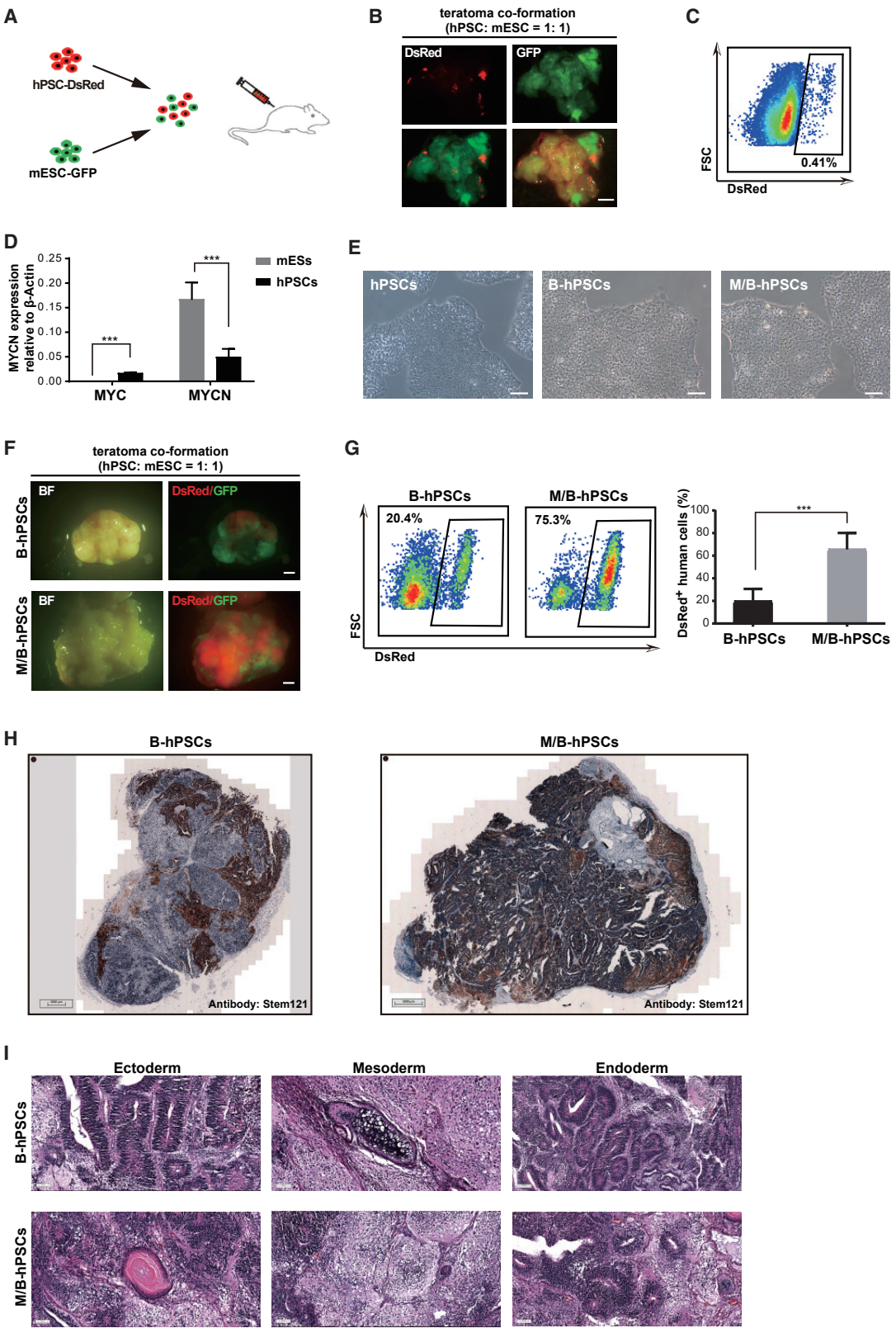

(legend on next page)

To investigate new strategies that enhance hPSC interspecies chimerism, we firstly set up a teratoma co-formation assay with mixed hPSCs and mouse ESCs (mPSCs), which to some extent mimic chimera development *in vivo*. We showed that hPSCs failed to co-differentiate with mESCs and contribute teratoma in the presence of mESCs. Overcoming apoptosis by BCL2 in hPSCs promoted their contribution rate from 0.5% to 20% in teratomas formed by a mixture with mESCs at the original 1:1 ratio. Combined with MYCN, a pro-growth factor (M/B) promoted the hPSC contribution rate to 75% in teratoma co-formed by hPSCs/mESCs. hPSCs expressing both BCL2 and MYCN (M/B-hPSCs) show robust integration into pre-implantation embryos of different species, such as mice, rabbits, and pigs. Strikingly, M/B-hPSCs injected into pre-implantation *Flk-1*$^{+/-}$ mouse embryos show further enhanced chimera efficiency that allows for obtaining live hPSC-derived CD34^{+} blood progenitor cells from chimeras through cell sorting. Thus, we provide proof of concept to obtain live and functional hPSC-derived cells through interspecies chimerism.

RESULTS

Promoting contribution of hPSCs in teratomas co-formed by hPSCs/mESCs

The embryonic-development timing is distinct between human and other species, such as mouse. To examine whether hPSCs and mESCs could differentiate normally in the presence of each other, we mixed differentially labeled hPSCs and mESCs in a 1:1 ratio for teratoma co-formation (Figures 1A–1C). The hPSC/mESC mixture formed typical teratomas after injection into immunodeficient mice (Figure 1B). However, the numbers of DsRed-labeled cells derived from hPSCs were very low in co-formed teratomas, accounting for fewer than 1% of all cells, while the majority of cells were GFP-labeled mESC-derived cells (Figures 1B–1C), indicating that hPSCs failed to differentiate normally in the presence of mESCs. Expressing BCL2 in hPSCs (Figures 1E and S1) to overcome potential apoptosis during teratoma formation only promotes their contribution rate up to around 20% in co-formed teratoma (Figures 1F–1H). To search additional factors to promote hPSC co-differentiation with mPSCs, we focus on MYC family genes, well-known factors that promote cell growth. *MYCN*, but not *C-MYC*, showed relatively higher expressions in mESCs compared with hPSCs (Figure 1D). Strikingly, *BCL2* combined with *MYCN* expression (M/B) promoted the hPSC contribution rate up to 70% in teratoma formed by hPSCs/mESCs (Figures 1E–1H and S1). Notably , immunohistochemical analysis and hematoxylin and eosin (H&E) staining showed three typical germ layers in teratomas formed by the mESC/B- or M/B-hPSC mixtures (Figures 1H and 1I). Together, these data demonstrate that BCL2 combined with MYCN enables enhanced differentiation of hPSCs in the presence of mESCs in a teratoma co-formation assay that might, to some extent, mimic chimera development *in vivo*.

M/B-hPSCs show enhanced integration and contribution in interspecies pre-implantation blastocysts

We and others have shown that primed hPSCs expressing anti-apoptotic factors such as BMI1 and BCL2 contribute to both extra-embryonic and embryonic lineages when injected into interspecies pre-implantation blastocysts (Wang et al., 2017b; Huang et al., 2018), but the overall efficiency is quite limited. To examine whether the combination of MYCN/BCL2 can further promote interspecies chimerism, we injected hPSCs expressing BCL2 (B-hPSCs) or M/B-hPSCs into 8-cell (8C)-stage mouse, pig, or rabbit embryos (Figure 2A). The integration of DsRed-labeled human cells was examined after 48–60 h of culture *in vitro*. M/B-hPSCs showed significantly higher cell numbers in mouse, pig, and rabbit embryos than B-hPSCs (Figures 2A–2B).

Figure 1. MYCN/BCL2 promotes the contribution of hPSCs in teratoma co-formation mixed with mESCs

(A) Schematic overview of co-differentiation of hPSCs-dsRed and mESCs-GFP *in vivo*. hPSCs-dsRed and mESCs-GFP are initially mixed in 1:1 ratio at the single-cell level for further differentiation.

(B and C) The teratoma formed by the mixture of hPSCs-dsRed and mESCs-GFP at 4 weeks. dsRed-labeled human cells in teratoma were analyzed by flow cytometry. Scale bars, 2 mm.

(D) Analysis of MYC and MYCN expression in the indicated cells by qRT-PCR. Error bars represent mean + SEM of three parallel experiments. ***$p < 0.001$.

(E) The morphology of BCL2- or MYCN/BCL2-expressed hPSCs. Scale bars, 100 μm.

(F) Teratomas formed by B-hPSCs or M/B-hPSCs mixed with mESCs in 1:1 ratio. Scale bars, 2 mm.

(G) Flow cytometry analysis of dsRed-labeled human cells in indicated teratomas. Error bars represent mean + SEM of three independent replicates. ***$p < 0.001$.

(H) Immunohistochemical analysis of human cells in indicated teratomas with human-specific anti-Stem121 antibody. Scale bars, 1 mm.

(I) H&E staining of teratomas formed by B-hPSCs or M/B-hPSCs mixed with mESCs in 1:1 ratio. Three typical germ layers are shown. Scale bars, 50 μm.

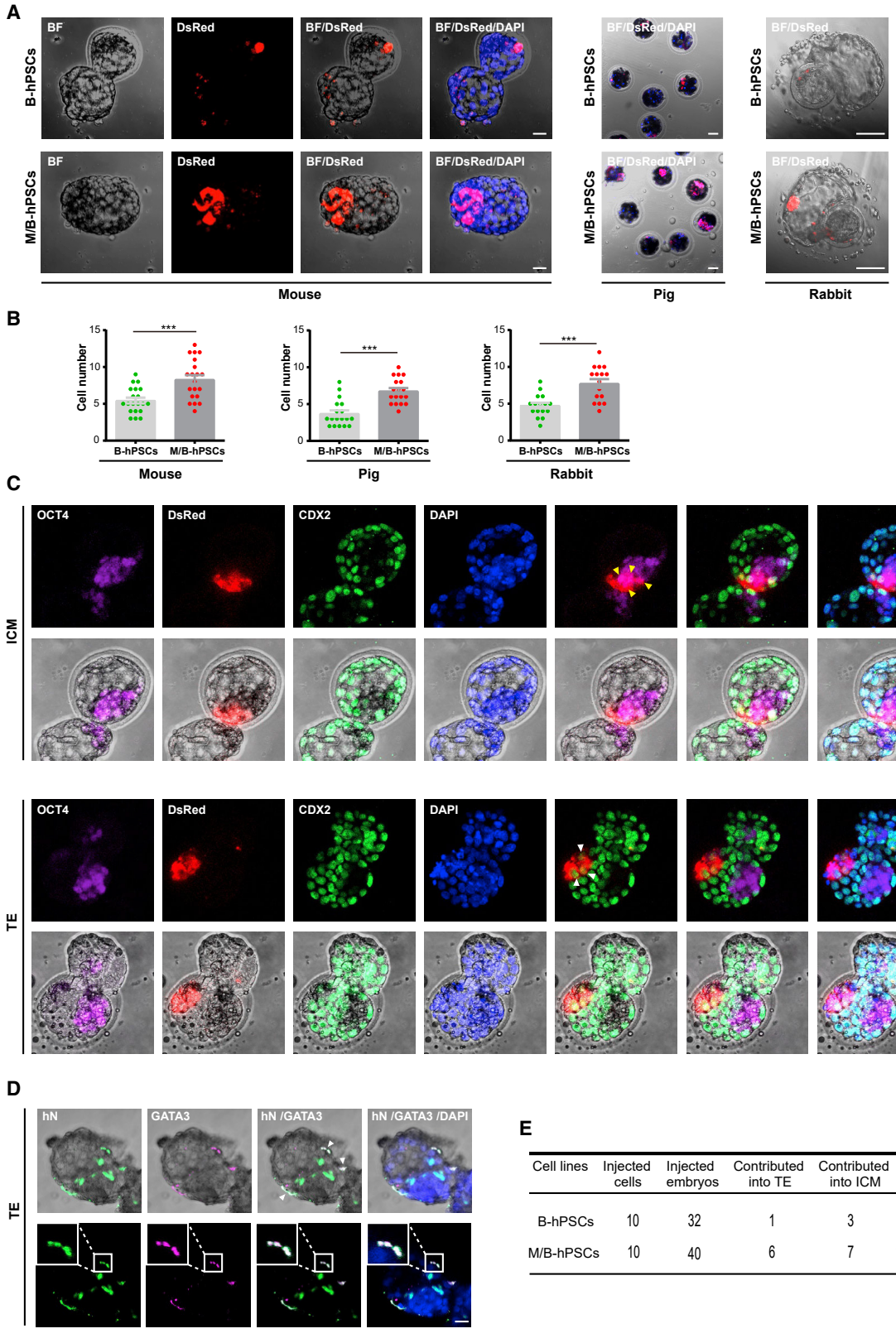

E

Cell lines	Injected cells	Injected embryos	Contributed into TE	Contributed into ICM	Total
B-hPSCs	10	32	1	3	4 (12.5%)
M/B-hPSCs	10	40	6	7	13 (32.5%)

(legend on next page)

We then examined the cell fate of these integrated hPSCs injected in mouse pre-implantation embryos. The extra-embryonic tissues (ExEms) as well as the inner cell mass (ICM) were then examined by co-immunostaining for the trophoblast marker CDX2 or GATA3 and the ICM marker OCT4 (Figures 2C and 2D). A considerable number of M/B-hPSCs were detected as CDX2/GATA3-or OCT4-positive when injected in mouse embryos, indicating that they contributed to both extra-embryonic and embryonic lineages (Figures 2C, 2D, and S3A). Moreover, M/B-hPSCs showed significantly higher efficiencies than B-hPSCs in terms of their lineage contributions in pre-implantation mouse blastocysts (Figure 2E). Overall, these data demonstrate that the combination of MYCN/BCL2 promotes interspecies chimerism of hPSCs in pre-implantation blastocysts of different species.

M/B-hPSCs show increased integration in mouse post-implantation chimera

We then examined the long-term chimeric contributions of M/B-hPSCs in mouse post-implantation embryonic day 10.5 (E10.5) conceptuses. First, by using a widely used human mitochondrial DNA (hmtDNA) qPCR assay with $1/10^4$ as a threshold, 70.8% of mouse embryos injected with M/B-hPSCs contained human cells, while only 21.1% of mouse embryos injected with B-hPSCs contained human cells (Figures 3A and 3B). Moreover, the M/B-hPSC contribution was detected in both extra-embryonic and embryonic lineages in recovered embryos (Figures 3A and S3B). In contrast, it is hard to detect B-hPSCs in contributing to both extra-embryonic and embryonic lineages in E10.5 chimeras (Figure 3B). To confirm the presence of human cells in chimera, we then examined human cells through immunostaining. We detected a considerable number of human cells at various embryonic regions in E10.5 mouse chimeras injected with dsRed-labeled M/B-hPSCs by immunostaining with the human-specific antibody Stem121 (Figures 3C and S3C). These cells differentiated into various morphologically distinct lineages at different embryonic regions in the mouse chimeras (Figures 3C and S3C). Furthermore, the dsRed+ cells in placenta tissue could be co-stained with Stem121 and antibody against CK7, a trophoblast marker (Figures S3D–S3E). In all, these data demonstrate that the combination of MYCN/BCL2 largely promotes the long-term integration of hPSCs in mouse post-implantation embryos.

M/B-hPSCs generate blood progenitor cells in *Flk-1* haplodeficient mouse embryos

Interspecies complementation using hPSCs is considered a promising approach to generate humanized functional cells or organs. During interspecies complementation, the injected PSCs are required to complement the deficient lineages in host embryos, which might in turn enhance their overall contribution rate in chimera. We then examined whether M/B-hPSCs could generate targeted cells in *Flk-1* impaired mouse embryos, which have severe defects in blood/endothelia lineages (Hamanaka et al., 2018; Wang et al., 2020). In this model, the mouse *Flk-1* gene locus was replaced with EGFP (*Flk-1*$^{+/EGFP}$) (Wang et al., 2020). dsRed-labeled M/B-hPSCs were injected into pre-implantation blastocysts that were generated by intercrossing *Flk-1*$^{+/EGFP}$ mice and analyzed at E10.5. Since the homozygous *Flk-1*$^{EGFP/EGFP}$ embryos failed to develop to E10.5, we just obtained and analyzed chimeras in *Flk-1*$^{+/EGFP}$ embryos in which the mouse endothelial lineage was labeled by EGFP (Figure 4A) (Wang et al., 2020). M/B-hPSC-derived cells were detectable in nearly 90% of *Flk-1*$^{+/EGFP}$ mouse chimeras (Figures 4B and 4C). Moreover, the overall contribution of human cells was significantly higher in *Flk-1*$^{+/EGFP}$ mouse chimeras compared with wild-type (WT) chimeras (Figures 3 and 4B). In some chimeras, the human cell ratios were above 1:1,000 or even 1:100 based on an hmtDNA qPCR assay (Figure 4B). Importantly, a number of live human CD34$^+$ hematopoietic/endothelial progenitor cells were detected in *Flk-1*$^{+/EGFP}$ mouse chimeras based on fluorescence-activated cell sorting (FACS) analysis (Figure 4D). These cells were successfully sorted and cultured *in vitro* (Figure 4E).

Figure 2. MYCN/BCL2 promotes the integration and proliferation of hPSCs in interspecies pre-implantation embryos

(A and B) Survival and proliferation of dsRed-labeled hPSCs in pre-implantation embryos of different species. dsRed + hPSCs (10 cells for mouse, 3–5 cells for pig, and 7 cells for rabbit) were injected into 8-cell (8C)-stage embryos of indicated species and were cultured for 3 days *in vitro*, and the cell number of each indicated cell line was calculated. Scale bars, 20 μm. Mouse: mean + SEM of 20 (+B) or 20 (+N + B) samples; pig: mean + SEM of 18 (+B) or 18 (+N + B) samples; rabbit: mean + SEM of 16 (+B) or 16 (+N + B) samples. ***$p < 0.001$.

(C) Contribution of hPSCs to embryonic and extra-embryonic embryonic lineages in mouse chimeras. Representative images showing the integration of M/B-hPSCs co-expressing OCT4, an ICM marker, or CDX2, an early trophoblast marker in cultured chimeric embryos. Yellow arrow, dsRed$^+$/OCT4$^+$ cells; white arrow, dsRed$^+$/CDX2$^+$ cells; scale bars, 20 μm.

(D) Representative images showing the integration of M/B-hPSC co-staining with hN (human cell nucleus-specific antibody) and GATA3 (early extra-embryonic lineage marker) in cultured chimeric embryos. White arrow, hN$^+$/GATA3$^+$ cells; scale bars, 20 μm.

(E) Summary of chimera assays with injection of ten indicated dsRed+ cells at the 8C-stage embryo, followed by 48–60 h *in vitro* development into the blastocyst stage.

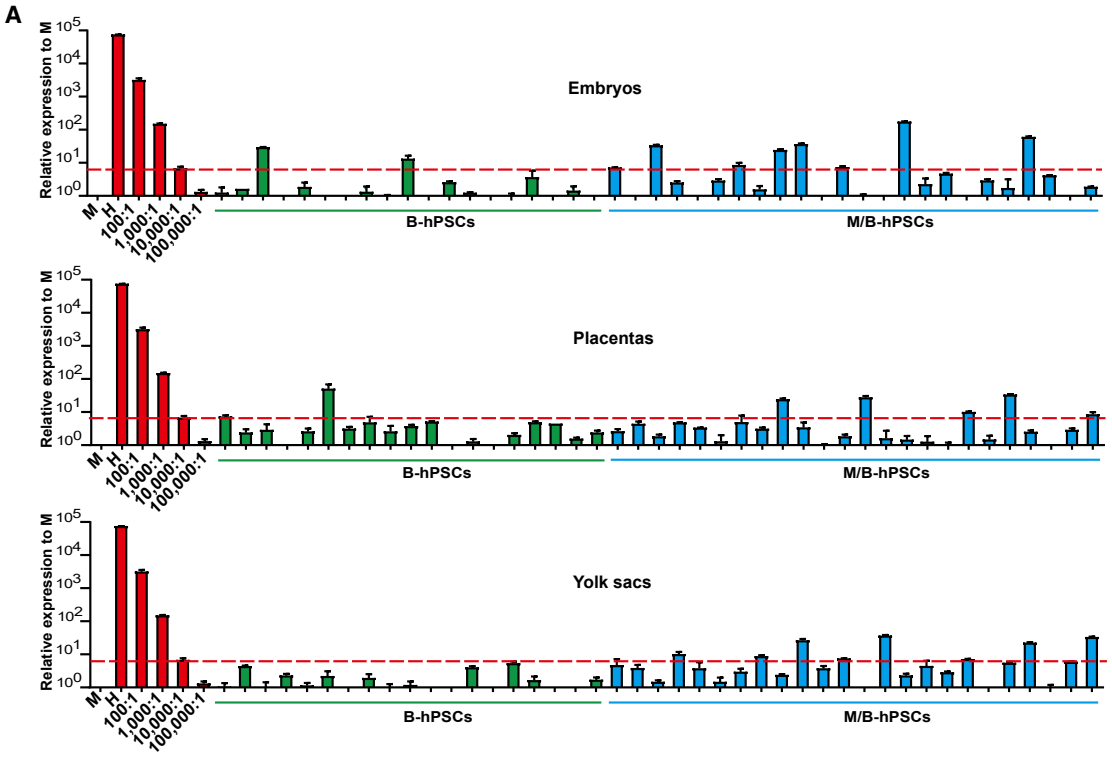

B

Cell lines	Stage of injection	Injected embryos	Dissected embryos	Contributed into Em	Contributed into ExEm	Contributed into both ExEm and Em	Total
B-hPSCs	Morula/ Blastocyst	62	19	2 (10.5%)	2 (10.5%)	0 (0%)	4 (21.1%)
M/B-hPSCs	Morula/ Blastocyst	82	24	8 (33.3%)	13 (54.2%)	4 (16.7%)	17 (70.8%)

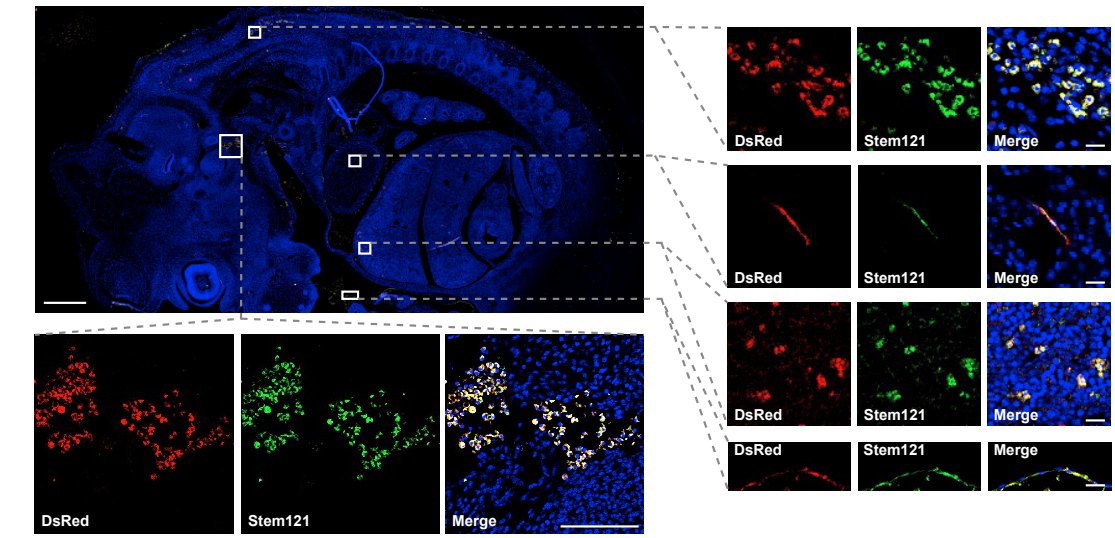

(legend on next page)

To examine the function of these chimera-derived human CD34$^+$ cells, we performed a colony-forming unit (CFU) assay (Figure 4F). Strikingly, CD34$^+$ human cells sorted from the chimeras successfully generated typical CFUs *in vitro* (Figure 4F). Further Giemsa staining of cells from these colonies showed morphologies of various blood lineages, such as macrophage, erythroid, monocyte, granulocyte, and other lineages (Figure 4G). Together, these data demonstrate that the chimerism-enhanced hPSCs generate functional blood progenitor cells in *Flk-1* haplodeficient mouse embryos.

DISCUSSION

Interspecies chimerism using hPSCs is hoped to generate xenogeneic organs or functional cells through animal blastocyst complementation. However, the concept has not been proved due to the extremely low efficiency of hPSCs in interspecies chimera. Even the "stage-matched" naive hPSCs still show very low and variable interspecies-chimera competence (Gafni et al., 2013; Masaki et al., 2015; Theunissen et al., 2016; Hu et al., 2020). In this study, we generated chimerism-enhanced hPSCs by combining an anti-apoptotic factor, BCL2, and a pro-growth factor, MYCN (M/B). M/B expression greatly promoted integration and growth of conventional hPSCs in pre-implantation blastocysts of different species such as mouse, rabbit, and pig, as well as in the post-implantation of mouse embryos. The chimera efficiency was further increased in *Flk-1* haplodeficient mouse embryos, indicating the context of complementation might enhance chimera formation. Importantly, we could sort the live human CD34$^+$ blood/endothelial progenitor cells from mouse chimera with M/B-hPSCs. These chimera-derived human CD34$^+$ progenitors further gave rise to various subtype blood cells in a CFU assay. To our knowledge, obtaining live and functional human cells from interspecies chimera has not been reported. Thus, our study proves the concept to generate functional human cells through enhanced interspecies chimerism with hPSCs.

The mechanism of the chimera barrier using hPSCs remains to be fully illustrated. We and others have reported that hPSCs undergo severe apoptosis after injection into animal pre-implantation blastocysts (Wang et al., 2017a, 2017b; Huang et al., 2018). Recently, Wu et al. reported a cell competition mechanism between hPSCs and host cells, leading to the death of hPSCs in chimera (Zheng et al., 2021). Indeed, hPSCs contributed very few cells in teratoma co-formation by the mixture containing mESCs (Figure 1). The failure of hPSCs to differentiate in the presence of mESCs might not be due to their "primed state" since hPSCs also underwent severe apoptosis in the presence of mouse-primed epiblast stem cells (mEpiSCs) (Figure S4A). The anti-apoptotic factor BCL2 did elevate the ratio of hPSC-derived cells in teratoma, but it was still much lower compared with mESC-derived cells (Figure 1). Interestingly, combined with another pro-growth factor, MYCN enables hPSCs dominating the teratoma co-formation with mESCs (Figure 1). Finally, BCL2 and MYCN successfully enhanced interspecies chimera in hPSCs, as observed in co-teratoma formation. Interestingly, MYCN factor was also reported to enhance cell competition in mouse early embryonic development, during which MYCN-high epiblast cells eliminated MYCN-low ones (Ellis et al., 2019). hPSCs indeed show relatively lower MYCN expressions compared with mESCs (Figure 1D), thus they might be eliminated during co-teratoma or chimera formation. Indeed, in a simple co-differentiation assay mixed by hPSCs and mESCs, hPSCs underwent rapid apoptosis and were eliminated (Figures S2 and S4D), while MYCN expression largely prevent cell death and promoted the growth of hPSCs during co-differentiation with mESCs (Figures S2E–S2H). hPSCs expressing MYCN or both BCL2 and MCYN exhibit normal morphology and differentiation potential in forming typical teratoma with normal three germ layers (Figure S1). Notably, BCL2 and MCYN could enable hPSCs to survival well in co-differentiation or teratoma formation mixed with mESCs in a very low ratio such as 1:30 (Figures S4B and S4C). However, just MYCN itself did not overcome apoptosis or enhance cloning efficiency in dissociated hPSCs, and it failed to promote hPSC integration in pig pre-implantation embryos (Figures S2I and

Figure 3. MYCN/BCL2 promotes long-term chimera of hPSCs in post-implantation mouse embryos

(A) Quantitative genomic PCR analysis of the human mitochondria DNA in E10.5 chimeras of mouse embryos, placentas, and yolk sacs injected with the indicated cells. A human DNA control (H), a mouse DNA control (M), and a series of human-mouse cell dilutions (1/100 to 1/100,000) were run in parallel to estimate the degree of human cell integration. The dashed line indicates the detection level of one human cell in 10,000 mouse cells. Error bars represent mean + SEM of three parallel experiments.

(B) Summary of mouse chimeras containing human cells. Embryos were recovered at E10.5 stage. ExEm, extra-embryonic tissues including both placentas and yolk sacs; Em, embryonic lineages.

(C) Analyses of human cells at different embryonic regions in E10.5 mouse chimera by immunofluorescence using human-specific marker Stem121. Scale bars, 500 μm (D, left), 20 μm (D, middle), 5 μm (D, right), 500 μm (E, left), and 100 μm (E, right).

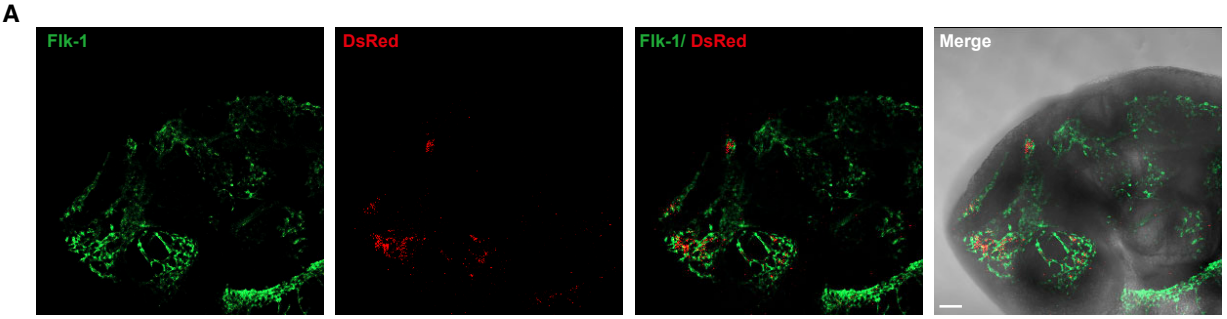

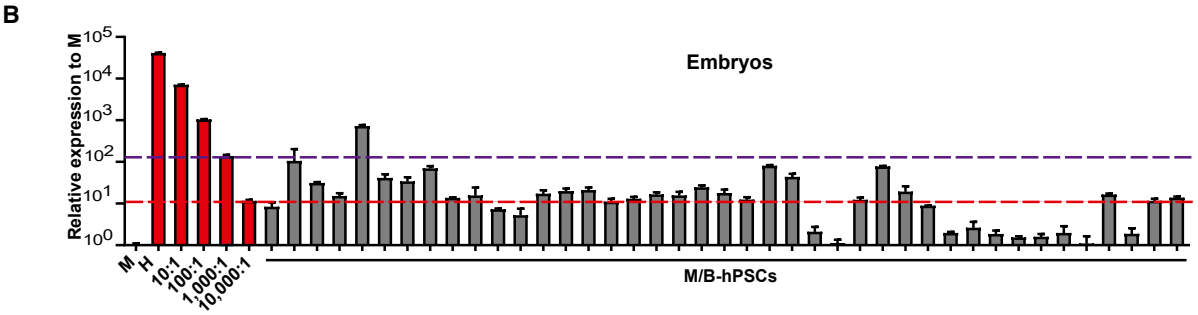

C

Cell lines	Stage of injection	Injected embryos	Dissected embryos	Contributed into Em	Contributed into ExEm	Contributed into both ExEm and Em	Total
M/B-hPSCs	Molura/ Blastocyst	150	41	26 (63.4%)	24 (58.5%)	15 (36.6%)	35 (85.4%)

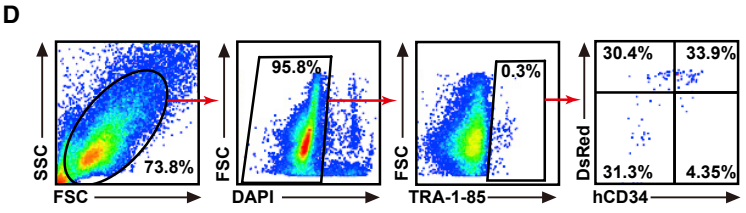

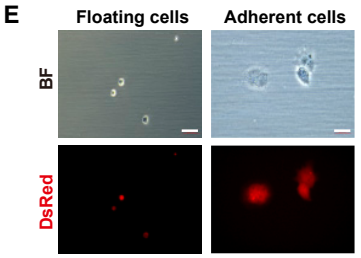

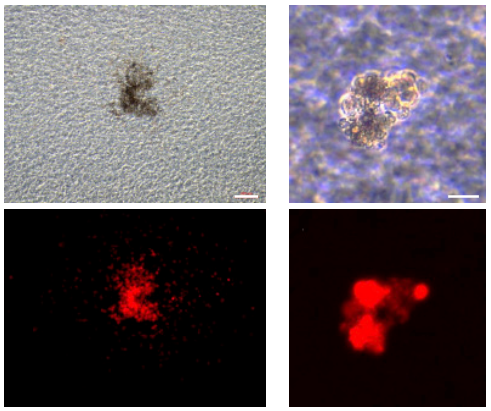

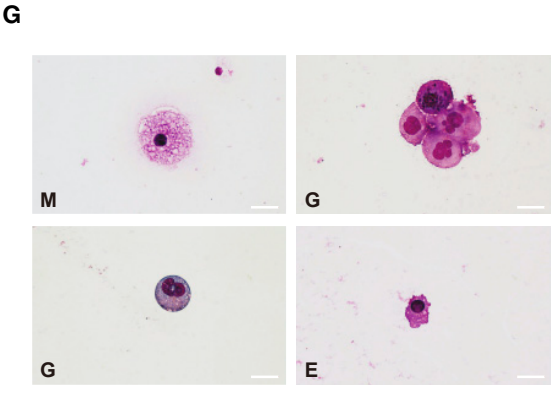

(legend on next page)

S2J). Thus, combining BCL2 and MYCN provides an enhanced approach for interspecies chimerism using hPSCs, which marks important progress by obtaining live and functional human cells through interspecies chimerism.

EXPERIMENTAL PROCEDURES

Culture and maintenance of hPSCs and mESCs

hPSCs were cultured under 20% O_2 and 5% CO_2 at 37°C conditions. The plates should be coated by Matrigel before use. hPSC lines UH10-dsRed, UH10-dsRed + MYCN, UH10-dsRed + BCl2, and UH10-dsRed + MYCN + BCl2 were maintained on plates with hPSC medium mTeSR1 (STEM CELL). Every 3 days, the hPSC lines were passaged using 0.5 mM ethylenediaminetetraacetic acid disodium salt (EDTA-2Na). All cell lines indicated above have been tested to be free of mycoplasma contamination. In particular, the generation of the UH10 hiPSCs was approved by the Institutional Review Board at Guangzhou Institutes of Biomedicine and Health. Also, we have complied with all relevant ethical regulations and obtained consent from human participants.

mESCs were cultured under 20% O_2 and 5% CO_2 at 37°C conditions. The plates should be coated by gelatin before use. mESCs were maintained in N2B27 + 2iL medium (50% DMEM/high glucose [Hyclone], 50% knockout DMEM [Gibco], N2 [Gibco, 200×] + B27 [Gibco, 100×], NEAA [Gibco, 100×], GlutaMAX [Gibco, 100×], sodium pyruvate [Gibco, 100×], 1 μM PD0325901 [Selleck], 3 μM CHIR99021 [Selleck], 100 μM β-mercaptoethanol [gibco], and 1,000 units mL^{-1} mLIF). Every 3 days, the mESCs were passaged using Accutase.

mEpiSCs were cultured under 20% O_2 and 5% CO_2 at 37°C conditions. The plates should be coated by serum before use. mEpiSCs were maintained in FN medium (50% F12/Neurobasal [Gibco], N2 [Gibco, 200×] + B27 [Gibco, 200×], NEAA [Gibco, 100×], GlutaMAX [Gibco, 100×], BSA [1 mg/mL], 100 μM β-mercaptoethanol [Gibco], activin A [20 ng/mL], and bFGF [20 ng/mL]). Every 3 days, the mEpiSCs were passaged using Accutase.

Generation of dsRed-labeled hPSCs and GFP-labeled mESCs

To construct UH10 hiPSCs with a constitutive expression of dsRed in the AAVS1 harbor locus, guide RNA (gRNA) for the AAVS1 safe harbor locus was designed on the CRISPR website (crispr.mit.edu) and cloned into pX330 (a vector that can express Cas9 protein and gRNA). Donor plasmid (pUC57-Neomycin-AAVS1-CAG-dsRed) contained left and right homology arms of the AAVS1 safe harbor locus. 1×10^6 hPSCs were electroporated with 4 μg donor plasmid and 2 μg pX330 plasmid, and dsRed+ cells were primarily selected by G418 (100 μg/mL) and then sorted by FACS. The GFPs were cloned into lentiviral vector Psin, and lentivirus was produced in 293T cells by co-transfection. Viral supernatants were collected at 48 h after transfection and passed through a 0.45 μm filter to remove cell debris then were subjected to ultracentrifugation (20,000 × *g* for 3 h at 4°C). mESCs were transduced with lentivirus, and the positive cells were selected by puromycin (1 μg/mL).

Generation of MYCN and BCl2 forced-expression hPSCs

The human MYCN and BCl2-2A-MYCN genes were cloned into a lentiviral vector tetO-FUW for tet-inducible expression of MYCN or co-expression MYCN and BCl2. Lentivirus was produced in 293T cells by co-transfecting the tetO-FUW-MYCN or tetO-FUW-BCl2-2A-MYCN with three helper plasmids (pRSV-REV, pMDLg/pRRE, and vesicular stomatitis virus G protein expression vector), which provide essential elements to package lentivirus. Viral supernatants were collected at 48 h after transfection and passed through a 0.45 μm filter to remove cell debris then were subjected to ultracentrifugation (20,000 × *g* for 3 h at 4°C). dsRed + hPSCs were transduced with lentivirus. The expression of MYCN and BCl2 were induced by an exogenous addition of doxycycline (DOX) (2 μg/per mL), and the positive cells were selected by puromycin (1 μg/mL).

Co-differentiation of hPSCs and mESCs

hPSCs and mESCs were dissociated into single cells and counted. For mono-layer co-differentiation *in vitro*, 1×10^5 hPSCs and

Figure 4. Generation of human CD34$^+$ endothelial/blood progenitor cells through interspecies chimera

(A) Representative fluorescence images showing the integration of human cells in the vascular regions of E10.5 *Flk-1*$^{+/EGFP}$ mouse chimeric embryos. Scale bars, 100 μm.

(B) Quantitative genomic PCR analysis of the human mitochondria DNA in E10.5 *Flk-1*$^{+/EGFP}$ mouse chimeras injected with M/B-hPSCs. A human DNA control (H), a mouse DNA control (M), and a series of human-mouse cell dilutions (1/100 to 1/100,000) were run in parallel to estimate the degree of human cell integration. The red and purple dashed lines indicate the detection level of one human cell in 10,000 and 1,000 mouse cells, respectively. Error bars represent mean + SEM of three parallel experiments.

(C) Summary of mouse chimeras containing human cells. Embryos were recovered and analyzed at the E10.5 stage. ExEm, extra-embryonic tissues including both placentas and yolk sacs; Em, embryonic lineages.

(D) Representative flow cytometry analysis of live human cells in E10.5 *Flk-1*$^{+/EGFP}$ mouse chimeric embryos. The antibody TRA-1-85 was used to identify human cells, and hCD34 was used to identify human endothelial and blood cells.

(E) The morphology of sorted live human cells (TRA-1-85$^+$). Scale bars, 100 μm.

(F) Representative pictures of CFUs formed by the sorted live human cells (TRA-1-85$^+$dsRed$^+$). To sort the cells for CFU assay, total cells from 10 embryos were pooled together, and roughly around 2,000 human TRA-1-85$^+$dsRed$^+$ cells were obtained. Around 1,000 human cells were seeded, and a total of 5 CFUs were detected. Scale bars, 200 μm (left) and 100 μm (right).

(G) May–Grunwald–Giemsa staining of different blood cells from (F). Scale bars, 20 μm. E, erythroid; G, granulocytes; M, macrophages.

1×10^5 mESCs were mixed and plated onto a Matrigel-coated 6-well plate. The control group contained only 1×10^5 hPSCs or mESCs. Cells were differentiated for 4 days in embryonic body (EB) differentiation medium (DMEM/F12 [Hyclone], 20% FBS, NEAA [1×, Gibco], GlutaMAX [1×, Gibco], and 0.1% beta-Mercaptoethanol [Gibco]). For mixed EB co-differentiation *in vitro*, 1×10^5 hPSCs and 1×10^5 mESCs were mixed and cultured with EB differentiation medium in a cell-culture flask. For mixed teratoma formation *in vivo*, 1×10^6 hPSCs and 1×10^6 mESCs were mixed and resuspended in 30% Matrigel (Corning) in DMEM/F12 (Hyclone) and then injected subcutaneously into NOD/SCID immunodeficient mice obtained from Beijing Vital River Laboratory Animal Technology. Teratomas were detected after 4 weeks. Mice were fed with the Dox-containing water (2 mg/mL) for inducible MYCN, BCl2, or MYCN-BCL2 expression.

Chimerism analysis

hPSCs were completely dissociated using Accutase and centrifuged at 300 × *g* at room temperature for 3 min. After removal of the supernatant, cells were resuspended in the culture medium at a proper density ($2–6 \times 10^5$ cells/mL) and placed on ice for 20–30 min before injection. For the *in vitro* extra-embryonic chimerism analysis, cells were microinjected into the 8C-stage embryos. Ten indicated dsRed+ cells were injected in mouse embryos, 3–5 indicated dsRed+ cells were injected in pig embryos, and 7 indicated dsRed+ cells were injected in rabbit embryos, while for the *in vivo* chimerism analysis, 10 indicated dsRed+ cells were microinjected into mouse later morulas or early blastocysts. For the *in vitro* chimerism assay, the injected embryos at the blastocyst stage were fixed by 4% PFA for 30 min and immunostianed (CDX2, OCT4, and DAPI). For chimerism analysis *in vivo*, embryos were harvested until E10.5 for an hmtDNA assay, FACS, or immunostaining.

CFU assay and cell morphology

The CFU assay was performed according to the manufacturer's instructions on Methocult H4435 (STEMCELL Technologies). Firstly, cells were suspended into 120 μL IMDM medium supplemented with 2% FBS (Biological Industries), and then add the cell suspension to 1 mL Methocult H4435. Next, transferred the mixture to 35 mm ultra-low attachment plates (STEMCELL Technologies) and rotated gently to spread methylcellulose medium over the surface of the dish. Three dishes were placed within a 100 mm Petri dish containing 3 mL sterile water and were incubated in 37°C, 20% O_2, and 5% CO_2 conditions. The CFUs were classified and calculated according to the morphology after 2 weeks. Then, harvested cells from the CFU assay were rinsed twice with DPBS (Gibco) and re-suspended in 200 μL DPBS. The morphology of cells was shown by microscopy after cytospin (500 × *g*, 3 min; cence) and stained with May–Grunwald–Giemsa.

Statistics

In general, data were presented as mean + SEM, and statistics were determined by unpaired two-tailed Student's test (t test). A p value <0.05 was considered statistically significant. *$p < 0.05$; **$p < 0.01$; ***$p < 0.001$. No statistical method was used to pre-determine the sample size. No samples were excluded for any analysis. No randomization was used for allocating the animal groups. No blinding was done in animal experiments.

Data and code availability

The datasets generated and/or analyzed during the current study are available from the corresponding author on reasonable request.

SUPPLEMENTAL INFORMATION

Supplemental information can be found online at https://doi.org/10.1016/j.stemcr.2022.03.009.

AUTHOR CONTRIBUTIONS

G.P., L.L., and Y.Z. designed the project and analyzed the data. G.P., Y.Z., and Z.Z. wrote the manuscript. Y.Z., Z.Z., and N.F. performed most experiments and analyzed the data. Z.Z., K.H., H.L., J.G., Q.Z., Z.O., Y.Y.S., C.L., and Jiaowei Wang performed the animal experiments. T.Z., J.T., and Junwei Wang assisted with FACS. J.T. and Y.Z. performed the qPCR assays. T.Z. performed karyotype analysis. Y.L.S. and Q.C. gave experiment suggestions or provided experiment materials for this research. All authors read and approved the final manuscript.

CONFLICTS OF INTEREST

The authors declare no competing interests.

ACKNOWLEDGMENTS

We thank the lab members in GIBH for their kindly help. This work was supported by the Strategic Priority Research Program of Chinese Academy of Sciences (grant no. XDA16030504); the National Natural Science Foundation of China (31971374, 32171451, and 32071454); the National Key Research and Development Program of China, Stem Cell and Translational Research (2017YFA0102600); the China Postdoctoral Science Foundation (2020M672589 and 2020T130134); the Science and Technology Planning Project of Guangdong Province, China (2020B1212060052); the Key Research & Development Program of Bioland Laboratory (Guangzhou Regenerative Medicine and Health Guangdong Laboratory) (2018GZR110104005); and the Guangdong Province Special Program for Outstanding Talents (to G.P., 2019JC05Y463).

Received: November 6, 2021
Revised: March 15, 2022
Accepted: March 15, 2022
Published: April 14, 2022

REFERENCES

Brons, I.G., Smithers, L.E., Trotter, M.W., Rugg-Gunn, P., Sun, B., Chuva de Sousa Lopes, S.M., Howlett, S.K., Clarkson, A., Ahrlund-Richter, L., Pedersen, R.A., et al. (2007). Derivation of pluripotent epiblast stem cells from mammalian embryos. Nature *448*, 191–195.

Buecker, C., Chen, H.H., Polo, J.M., Daheron, L., Bu, L., Barakat, T.S., Okwieka, P., Porter, A., Gribnau, J., Hochedlinger, K., et al.

(2010). A murine ESC-like state facilitates transgenesis and homologous recombination in human pluripotent stem cells. Cell Stem Cell *6*, 535–546.

Chan, Y.S., Goke, J., Ng, J.H., Lu, X.Y., Gonzales, K.A.U., Tan, C.P., Tng, W.Q., Hong, Z.Z., Lim, Y.S., and Ng, H.H. (2013). Induction of a human pluripotent state with distinct regulatory circuitry that resembles preimplantation epiblast. Cell Stem Cell *13*, 663–675.

Das, S., Koyano-Nakagawa, N., Gafni, O., Maeng, G., Singh, B.N., Rasmussen, T., Pan, X., Choi, K.D., Mickelson, D., Gong, W., et al. (2020). Generation of human endothelium in pig embryos deficient in ETV2. Nat. Biotechnol. *38*, 297–302.

Ellis, S.J., Gomez, N.C., Levorse, J., Mertz, A.F., Ge, Y., and Fuchs, E. (2019). Distinct modes of cell competition shape mammalian tissue morphogenesis. Nature *569*, 497–502.

Gafni, O., Weinberger, L., Mansour, A.A., Manor, Y.S., Chomsky, E., Ben-Yosef, D., Kalma, Y., Viukov, S., Maza, I., Zviran, A., et al. (2013). Derivation of novel human ground state naive pluripotent stem cells. Nature *504*, 282–286.

Guo, G., von Meyenn, F., Santos, F., Chen, Y.Y., Reik, W., Bertone, P., Smith, A., and Nichols, J. (2016). Naive pluripotent stem cells derived directly from isolated cells of the human inner cell mass. Stem Cell Rep. *6*, 437–446.

Hamanaka, S., Umino, A., Sato, H., Hayama, T., Yanagida, A., Mizuno, N., Kobayashi, T., Kasai, M., Suchy, F.P., Yamazaki, S., et al. (2018). Generation of vascular endothelial cells and hematopoietic cells by blastocyst complementation. Stem Cell Rep. *11*, 988–997.

Hanna, J., Cheng, A.W., Saha, K., Kim, J., Lengner, C.J., Soldner, F., Cassady, J.P., Muffat, J., Carey, B.W., and Jaenisch, R. (2010). Human embryonic stem cells with biological and epigenetic characteristics similar to those of mouse ESCs. Proc. Natl. Acad. Sci. U S A *107*, 9222–9227.

Hu, Z., Li, H., Jiang, H., Ren, Y., and Feng, J. (2020). Transient inhibition of mTOR in human pluripotent stem cells enables robust formation of mouse-human chimeric embryos. Sci. Adv. *6*, eaaz0298.

Huang, K., Zhu, Y., Ma, Y., Zhao, B., Fan, N., Li, Y., Song, H., Chu, S., Ouyang, Z., Zhang, Q., et al. (2018). BMI1 enables interspecies chimerism with human pluripotent stem cells. Nat. Commun. *9*, 4649.

Huang, Y., Osorno, R., Tsakiridis, A., and Wilson, V. (2012). In Vivo differentiation potential of epiblast stem cells revealed by chimeric embryo formation. Cell Rep. *2*, 1571–1578.

Isotani, A., Hatayama, H., Kaseda, K., Ikawa, M., and Okabe, M. (2011). Formation of a thymus from rat ES cells in xenogeneic nude mouse <-> rat ES chimeras. Genes Cells *16*, 397–405.

James, D., Noggle, S.A., Swigut, T., and Brivanlou, A.H. (2006). Contribution of human embryonic stem cells to mouse blastocysts. Dev. Biol. *295*, 90–102.

Kobayashi, T., Yamaguchi, T., Hamanaka, S., Kato-Itoh, M., Yamazaki, Y., Ibata, M., Sato, H., Lee, Y.-S., Usui, J.-i., Knisely, A.S., et al. (2010). Generation of rat pancreas in mouse by interspecific blastocyst injection of pluripotent stem cells. Cell *142*, 787–799.

Kojima, Y., Kaufman-Francis, K., Studdert, J.B., Steiner, K.A., Power, M.D., Loebel, D.A., Jones, V., Hor, A., de Alencastro, G., Logan, G.J., et al. (2014). The transcriptional and functional properties of mouse epiblast stem cells resemble the anterior primitive streak. Cell Stem Cell *14*, 107–120.

Masaki, H., Kato-Itoh, M., Umino, A., Sato, H., Hamanaka, S., Kobayashi, T., Yamaguchi, T., Nishimura, K., Ohtaka, M., Nakanishi, M., et al. (2015). Interspecific in vitro assay for the chimera-forming ability of human pluripotent stem cells. Development *142*, 3222–3230.

Mascetti, V.L., and Pedersen, R.A. (2016). Contributions of mammalian chimeras to pluripotent stem cell Research. Cell Stem Cell *19*, 163–175.

Takashima, Y., Guo, G., Loos, R., Nichols, J., Ficz, G., Krueger, F., Oxley, D., Santos, F., Clarke, J., Mansfield, W., et al. (2014). Resetting transcription factor control circuitry toward ground-state pluripotency in human. Cell *158*, 1254–1269.

Tesar, P.J., Chenoweth, J.G., Brook, F.A., Davies, T.J., Evans, E.P., Mack, D.L., Gardner, R.L., and McKay, R.D.G. (2007). New cell lines from mouse epiblast share defining features with human embryonic stem cells. Nature *448*, 196–U110.

Theunissen, T.W., Friedli, M., He, Y., Planet, E., O'Neil, R.C., Markoulaki, S., Pontis, J., Wang, H., Iouranova, A., Imbeault, M., et al. (2016). Molecular criteria for defining the naive human pluripotent state. Cell Stem Cell *19*, 502–515.

Theunissen, T.W., Powell, B.E., Wang, H., Mitalipova, M., Faddah, D.A., Reddy, J., Fan, Z.P., Maetzel, D., Ganz, K., Shi, L., et al. (2014). Systematic identification of culture conditions for induction and maintenance of naive human pluripotency. Cell Stem Cell *15*, 471–487.

Thomson, J.A., Itskovitz-Eldor, J., Shapiro, S.S., Waknitz, M.A., Swiergiel, J.J., Marshall, V.S., and Jones, J.M. (1998). Embryonic stem cell lines derived from human blastocysts. Science *282*, 1145–1147.

Wang, W.Q., Zhu, Y.L., Huang, K., Shan, Y.L., Du, J., Dong, X.Y., Ma, P., Wu, P.F., Zhang, J., Huang, W.H., et al. (2017a). Suppressing P16(Ink4a) and P14(ARF) pathways overcomes apoptosis in individualized human embryonic stem cells. Faseb J. *31*, 1130–1140.

Wang, X., Li, T., Cui, T., Yu, D., Liu, C., Jiang, L., Feng, G., Wang, L., Fu, R., Zhang, X., et al. (2017b). Human embryonic stem cells contribute to embryonic and extraembryonic lineages in mouse embryos upon inhibition of apoptosis. Cell Res. *28*, 126–129.

Wang, X., Shi, H., Zhou, J., Zou, Q., Zhang, Q., Gou, S., Chen, P., Mou, L., Fan, N., Suo, Y., et al. (2020). Generation of rat blood vasculature and hematopoietic cells in rat-mouse chimeras by blastocyst complementation. J. Genet. Genomics *47*, 249–261.

Ware, C.B., Nelson, A.M., Mecham, B., Hesson, J., Zhou, W.Y., Jonlin, E.C., Jimenez-Caliani, A.J., Deng, X.X., Cavanaugh, C., Cook, S., et al. (2014). Derivation of naive human embryonic stem cells. Proc. Natl. Acad. Sci. U S A *111*, 4484–4489.

Wu, J., Platero-Luengo, A., Sakurai, M., Sugawara, A., Antonia Gil, M., Yamauchi, T., Suzuki, K., Bogliotti, Y.S., Cuello, C., Valencia, M.M., et al. (2017). Interspecies chimerism with mammalian pluripotent stem cells. Cell *168*, 473–486.

Zheng, C., Hu, Y., Sakurai, M., Pinzon-Arteaga, C.A., Li, J., Wei, Y., Okamura, D., Ravaux, B., Barlow, H.R., Yu, L., et al. (2021). Cell competition constitutes a barrier for interspecies chimerism. Nature *592*, 272–276.